Rotation of the trajectories of bright solitons and realignment of intensity distribution in the coupled nonlinear Schrödinger equation

R. Radha,[1,*] P. S. Vinayagam,[1] and K. Porsezian[2,†]
[1]Centre for Nonlinear Science, PG and Research Department of Physics, Government College for Women (Autonomous), Kumbakonam 612001, India
[2]Department of Physics, Pondicherry University, Pondicherry 605014, India
(Received 1 May 2013; published 3 September 2013)

We reconsider the collisional dynamics of bright solitons in the coupled nonlinear Schrödinger equation. We observe that apart from the intensity redistribution in the interaction of bright solitons, one also witnesses a rotation of the trajectories of bright solitons. The angle of rotation can be varied by suitably manipulating the self-phase-modulation (SPM) or cross-phase-modulation (XPM) parameters. The rotation of the trajectories of the bright solitons arises due to the excess energy that is injected into the dynamical system through SPM or XPM. This extra energy contributes not only to the rotation of the trajectories, but also to the realignment of intensity distribution between the two modes. We also notice that the angular separation between the bright solitons can also be maneuvered suitably. The above results, which exclude quantum superposition for the field vectors, may have wider ramifications in nonlinear optics, Bose-Einstein condensates, and left- and right-handed metamaterials.

DOI: 10.1103/PhysRevE.88.032903 PACS number(s): 05.45.Yv, 42.81.Dp, 42.65.Tg

I. INTRODUCTION

The potential of solitons to carry information in optical fibers, which was theoretically predicted by Hasegawa and Tappert [1] in 1973, was experimentally realized in 1980 by Mollenauer *et al*. [2]. Since then, the propagation of temporal optical solitons in long-distance optical fiber communication and optical switching devices [3] has been investigated. Mathematically speaking, the propagation of an electromagnetic wave through a single-mode optical fiber when the Kerr nonlinearity [self-phase-modulation (SPM)] exactly counterbalances the group velocity dispersion is governed by an integrable "soliton" possessing nonlinear Schrödinger (NLS) equation [1,3]. A single-mode fiber can also support two orthogonal directions. Under ideal conditions of perfect cylindrical geometry and an isotropic material, a mode excited with its polarization in one particular direction would not couple to the mode with the orthogonal state. However, in practice, small departures from cylindrical geometry or small fluctuations in material anisotropy result in mixing up of the two polarization states, thereby breaking the mode degeneracy [4]. In conventional single-mode fibers, birefringence is not a constant parameter along the fiber but changes randomly because of fluctuations in the core shape and stress-induced anisotropy. Thus, it is clear that when two or more optical waves copropagate inside a fiber, they interact with each other through the fiber nonlinearity. This provides a coupling between the incident waves through the phenomenon called cross-phase-modulation (XPM). XPM occurs because the effective refractive index of a wave depends not only on the intensity of that wave, but also on the intensity of the copropagating wave. XPM is always accompanied by SPM. When the two waves have orthogonal polarizations, the XPM-caused coupling induces a nonlinear birefringence in the fiber. Hence, the propagation of solitons through nonlinear birefringent fibers is governed by coupled NLS equations [5] of the form

$$iq_{1t} + q_{1xx} + 2(g_{11}|q_1|^2 + g_{12}|q_2|^2)q_1 = 0, \quad \text{(1a)}$$

$$iq_{2t} + q_{2xx} + 2(g_{21}|q_1|^2 + g_{22}|q_2|^2)q_2 = 0, \quad \text{(1b)}$$

where $q_i(x,t)$ $(i = 1,2)$ are the envelopes of the field components. In the above equation, g_{11} and g_{22} account for the strengths of self-phase-modulation while g_{12} and g_{21} represent the strengths of cross-phase-modulation. It has been found that Eq. (1) is integrable if either (i) $g_{11} = g_{12} = g_{21} = g_{22}$ or (ii) $g_{11} = g_{21} = -g_{12} = -g_{22}$. The first choice corresponds to the Manakov model [4,6–10] which has been investigated [7,8] and the intensity redistribution of the bright solitons identified. The second choice corresponds to the modified Manakov model [9,10] and its soliton dynamics has been explored. Bright solitons that are the localized solutions of the coupled NLS equations (1) continue to attract the attention of researchers even today in nonlinear optics [11] and Bose-Einstein condensates (BECs) [12]. While it has been shown that soliton radiation trapping occurs due to cross-phase-modulation in the former case, vector soliton out-coupling occurs due to the intra(interspecies) scattering lengths in the latter case. However, it should be mentioned that since the solitons lie in the high-kinetic-energy regime [13], quantum superposition is forbidden.

In addition to the above physical interpretation, for handling more channels at high bit rate, it is necessary to achieve wavelength division multiplexing (WDM) [3] using coupled nonlinear Schrödinger equations through optical soliton transmission. This is possible by propagation through different channels with different carrier frequencies. In either case, two or more fields are to be propagated in the fiber. Hence, the dynamics of the fiber system is governed by the above coupled system of equations which are not integrable in general. In addition, the dynamics of higher-order coupled NLS equations including the third-order dispersion, Kerr dispersion, and

*radha_ramaswamy@yahoo.com
†ponzsol@yahoo.com

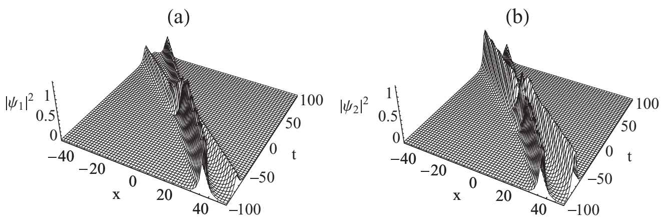

FIG. 1. Intensity distribution in the coupled NLS equations for the parametric choice $a = 1$, $b = 1$, $\varepsilon_1^{(1)} = 0.85i$, and $\varepsilon_1^{(2)} = 0.5$.

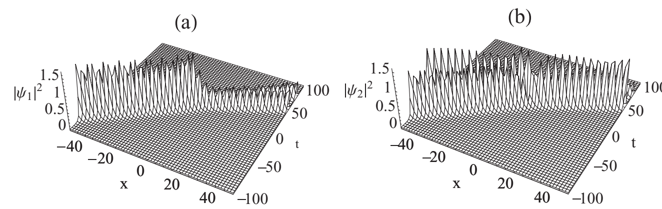

FIG. 3. Realignment of intensity distribution for the parametric choice $a = 1.5$, $b = 1.5$, $\varepsilon_1^{(1)} = 0.85i$, and $\varepsilon_1^{(2)} = 0.5$.

stimulated Raman scattering has also been analyzed [14]. In addition to the above situations, coupling is also possible in a system of two parallel waveguides coupled through evanescent field overlap, the coupling of two polarization modes in uniform guides, nonlinear optical waveguide arrays, and nonlinear distributed feedback structures [3]. Also, nonlinear couplers use solitons as ideal tools for performing all-optical switching operations [15].

At this juncture, it should be mentioned that the coupled NLS and coupled higher-order NLS type equations discussed above have been associated with the concept of intensity redistribution of solitons, a property which has wider ramifications in optical fiber communications such as providing intensity pump sources, soliton switching [15], etc. Can one identify other properties or signatures of the coupled NLS or NLS type equations which could come in handy in the propagation of solitons in optical fibers? The answer to this question assumes great significance for improving the efficiency of soliton-based communication systems. In the present paper, we unearth some additional signatures of coupled NLS equations, which include the rotation of the trajectories of bright solitons, realignment of intensity distribution between the two modes, and the variation of angular separation between the bright solitons. We show that all the above occur at the expense of additional energy pumped into the dynamical system by virtue of the variation of SPM and XPM.

II. BRIGHT SOLITONS AND THEIR COLLISIONAL DYNAMICS

Invoking the constraint $g_{11} = g_{12} = g_{21} = g_{22}$ or $g_{11} = g_{21} = -g_{12} = -g_{22}$, Eq. (1) can be linearized as

$$\Phi_x + U\Phi = 0, \tag{2}$$

$$\Phi_t + V\Phi = 0, \tag{3}$$

where $\Phi = (\phi_1, \phi_2, \phi_3)^T$ and

$$U = \begin{pmatrix} -2i\zeta & \sqrt{a}\psi_1 & \sqrt{b}\psi_2 \\ \sqrt{a}\psi_1^* & i\zeta & 0 \\ \sqrt{b}\psi_2^* & 0 & i\zeta \end{pmatrix}, \tag{4}$$

$$V = \begin{pmatrix} -(B+J) & A & K \\ A^* & B & G \\ K^* & H & J \end{pmatrix}, \tag{5}$$

with

$$A = i\sqrt{a}\psi_{1x} + 3\sqrt{a}\zeta\psi_1,$$
$$K = i\sqrt{b}\psi_{2x} + 3\sqrt{b}\zeta\psi_2,$$
$$A^* = -\sqrt{a}i\psi_{1x}^* + 3\sqrt{a}\zeta\psi_1^*,$$
$$K^* = -\sqrt{b}i\psi_{2x}^* + 3\sqrt{b}\zeta\psi_2^*,$$
$$B = 3i\zeta^2 + ia\psi_1\psi_1^*,$$
$$J = 3i\zeta^2 + ib\psi_2\psi_2^*,$$
$$G = i\sqrt{a}\sqrt{b}\psi_2\psi_1^*,$$
$$H = i\sqrt{a}\sqrt{b}\psi_1\psi_2^*,$$

where $\zeta = \mu ab$ and μ is the so called "hidden complex isospectral parameter," while a and b are real parameters. The compatibility condition $U_t - V_x + [U,V] = 0$ generates the following equations:

$$i\psi_{1t} + \psi_{1xx} + 2(a|\psi_1|^2 + b|\psi_2|^2)\psi_1 = 0, \tag{6a}$$

$$i\psi_{2t} + \psi_{2xx} + 2(a|\psi_1|^2 + b|\psi_2|^2)\psi_2 = 0. \tag{6b}$$

The above equations, when $a = b$, reduce to the Manakov model [7,8] while for $a = -b$, one obtains the modified Manakov model [9,10].

To generate the bright vector solitons of the above coupled nonlinear Schrödinger equations (6), we now consider the

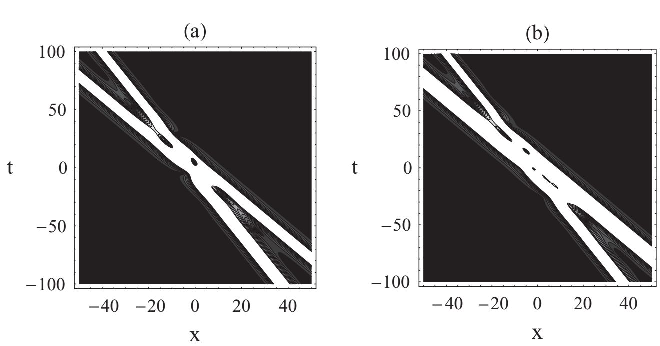

FIG. 2. Trajectories of bright solitons in the two modes.

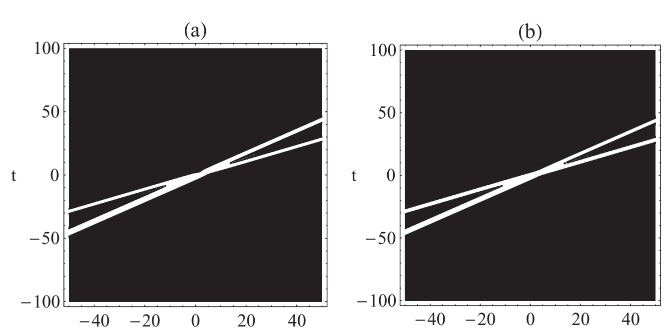

FIG. 4. Rotation of the trajectories of bright solitons.

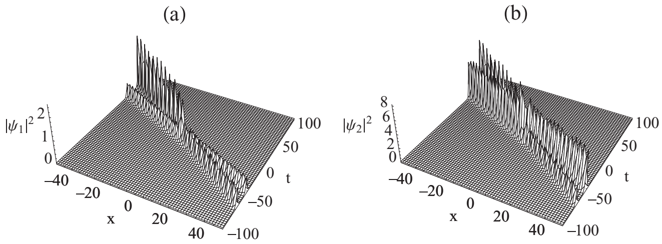

FIG. 5. Further realignment of intensity distribution for the choice $a = 2.5$, $b = 2.5$, $\varepsilon_1^{(1)} = 0.85i$, and $\varepsilon_1^{(2)} = 0.5$.

vacuum solution ($\psi_1^{(0)} = \psi_2^{(0)} = 0$) and employ the gauge transformation approach [16] to obtain the bright soliton solutions in the following form:

$$\psi_1^{(1)} = \varepsilon_1^{(1)}\beta_1 \operatorname{sech}(\theta_1)e^{i(-\xi_1)}, \tag{7}$$

$$\psi_2^{(1)} = \varepsilon_2^{(1)}\beta_1 \operatorname{sech}(\theta_1)e^{i(-\xi_1)}, \tag{8}$$

where

$$\theta_1 = 2\beta_1 x + 8\alpha_1\beta_1 t - 2\delta_1,$$
$$\xi_1 = 2\alpha_1 x + 4\left(\alpha_1^2 - \beta_1^2\right)t - 2\chi_1,$$

with $\alpha_1 = \alpha_{10}ab$, $\beta_1 = \beta_{10}ab$, while $\zeta_1 = \alpha_1 + i\beta_1$ and $\bar{\zeta}_1 = \zeta_1^*$. In the above equation, δ_1 and χ_1 are arbitrary parameters while $\varepsilon_{1,2}$ represent coupling parameters.

From the bright soliton solution, one understands that their amplitude depends not only on the coupling parameters $\varepsilon_1^{(1)}$ and $\varepsilon_2^{(1)}$, but also on the self-phase-modulation and cross-phase-modulation parameters a and b. This means that the impact of self-phase-modulation and cross-phase-modulation can be represented suitably in the collisional dynamics of bright solitons.

To understand the impact of SPM and XPM in the coupled NLS equations, we now consider the two-soliton solution obtained by employing the gauge transformation approach [16] in the following form:

$$\psi_1^{(2)} = \psi_1^{(1)} - 2i(\zeta_2 - \bar{\zeta}_2)\frac{\tilde{P}_{12}}{R}, \tag{9}$$

$$\psi_2^{(2)} = \psi_2^{(1)} - 2i(\zeta_2 - \bar{\zeta}_2)\frac{\tilde{P}_{13}}{R}, \tag{10}$$

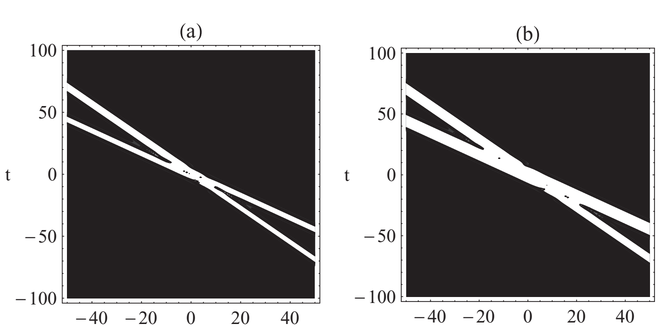

FIG. 6. Enhanced rotation of the trajectories of bright solitons.

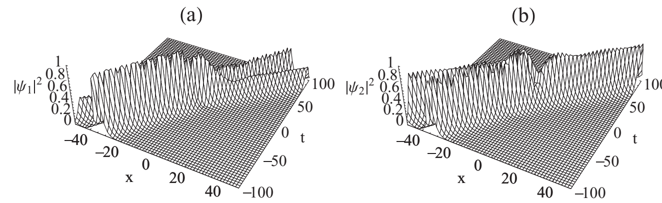

FIG. 7. Collisional dynamics of bright solitons for the modified coupled NLS equations for $a = -b = 0.9$, and $\varepsilon_1^{(1)} = 0.85i$, $\varepsilon_1^{(2)} = 0.5$.

where $\zeta_2 = \bar{\zeta}_2 = \alpha_2 + i\beta_2$. The explicit forms of $\tilde{P}_{12}$ and $\tilde{P}_{13}$ are given by

$$\begin{aligned}
\tilde{P}_{12}^1 = -\{&M_{12}^{(1)}[(\tau + \gamma M_{11}^{(1)})M_{11}^{(2)} + \gamma(M_{12}^{(1)}M_{21}^{(2)}\gamma^*/\tau^2\\
&+ M_{13}^{(1)}M_{31}^{(2)})] + M_{32}^{(1)}[(\tau + \gamma M_{11}^{(1)})M_{13}^{(2)}\\
&+ \gamma(M_{12}^{(1)}M_{23}^{(2)} + M_{13}^{(1)}M_{33}^{(2)})]\gamma^*/\tau^2\\
&+ [(\tau + \gamma M_{11}^{(1)})M_{12}^{(2)} + \gamma(M_{12}^{(1)}M_{22}^{(2)} + M_{13}^{(1)}M_{32}^{(2)})]\\
&\times(\tau + M_{22}^{(1)}\gamma^*)/\tau^2\},\\
\tilde{P}_{13}^1 = -\{&M_{13}^{(1)}[(\tau + \gamma M_{11}^{(1)})M_{11}^{(2)} + \gamma(M_{12}^{(1)}M_{21}^{(2)}\\
&+ M_{13}^{(1)}M_{31}^{(2)})]\gamma^*/\tau^2 + M_{23}^{(1)}[(\tau + \gamma M_{11}^{(1)})M_{12}^{(2)}\\
&+ \gamma(M_{12}^{(1)}M_{22}^{(2)} + M_{13}^{(1)}M_{32}^{(2)})]\gamma^*/\tau^2\\
&+ [(\tau + \gamma M_{11}^{(1)})M_{13}^{(2)} + \gamma(M_{12}^{(1)}M_{23}^{(2)} + M_{13}^{(1)}M_{33}^{(2)})]\\
&\times(\tau + M_{33}^{(1)}\gamma^*)/\tau^2\},
\end{aligned}$$

and

$$\tau = M_{11}^{(1)} + M_{22}^{(1)} + M_{33}^{(1)}, \qquad \gamma = \frac{\lambda_1 - \mu_1}{\mu_2 - \lambda_1},$$
$$R = \tilde{P}_{11}^1 + \tilde{P}_{22}^1 + \tilde{P}_{33}^1, \qquad \gamma^* = -\frac{\lambda_1 - \mu_1}{\lambda_2 - \mu_1},$$

with

$$\begin{aligned}
\tilde{P}_{11}^1 = &M_{21}^{(1)}[(\tau + \gamma M_{11}^{(1)})M_{12}^{(2)} + \gamma(M_{12}^{(1)}M_{22}^{(2)}\\
&+ M_{13}^{(1)}M_{32}^{(2)})]\gamma^*/\tau^2 + M_{31}^{(1)}[(\tau + \gamma M_{11}^{(1)})M_{13}^{(2)}\\
&+ \gamma(M_{12}^{(1)}M_{23}^{(2)} + M_{13}^{(1)}M_{33}^{(2)})]\gamma^*/\tau^2\\
&+ [(\tau + \gamma M_{11}^{(1)})M_{11}^{(2)} + \gamma(M_{12}^{(1)}M_{21}^{(2)} + M_{13}^{(1)}M_{31}^{(2)})]\\
&\times(\tau + M_{11}^{(1)}\gamma^*)/\tau^2,
\end{aligned}$$

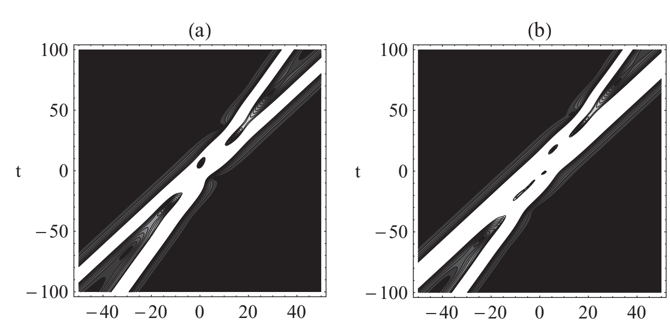

FIG. 8. Diagonally opposite trajectories of bright solitons in the modified coupled NLS equations.

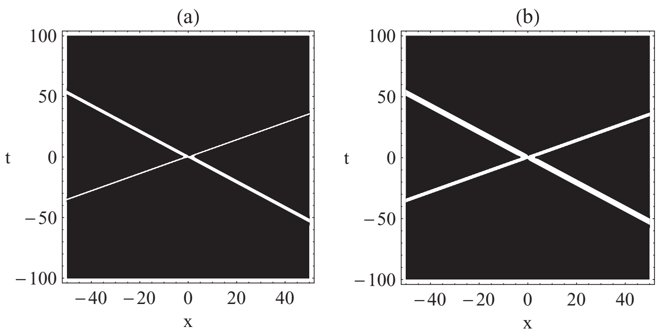

FIG. 9. Enhancement of angular separation between the solitons by varying μ_i, $i = 1,2$, for $\alpha_{10} = -0.1$, $\beta_{10} = -0.2$, $\alpha_{20} = 0.15$, $\beta_{20} = 0.3$ with the other parameters as in Fig. 3.

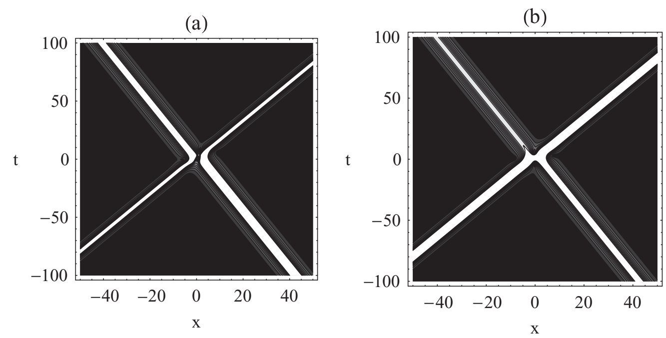

FIG. 10. Further enhancement of angular separation between the solitons for $\alpha_{10} = -0.1$, $\beta_{10} = -0.25$, $\alpha_{20} = 0.2$, $\beta_{20} = 0.3$ with the other parameters as in Fig. 3.

$$\begin{aligned}
\tilde{P}^1_{22} = {}& M^{(1)}_{12}\big[\gamma M^{(2)}_{11} M^{(1)}_{21} + M^{(2)}_{21}\big(\tau + \gamma M^{(1)}_{22}\big) \\
&+ \gamma M^{(1)}_{23} M^{(2)}_{31}\big]\gamma^*/\tau^2 + M^{(1)}_{32}\big[\gamma M^{(2)}_{13} M^{(1)}_{21} \\
&+ \big(\tau + \gamma M^{(1)}_{22}\big) M^{(2)}_{23} + \gamma M^{(1)}_{23} M^{(2)}_{33}\big]\gamma^*/\tau^2 \\
&+ \big[\gamma M^{(2)}_{12} M^{(1)}_{21} + \big(\tau + \gamma M^{(1)}_{22}\big) M^{(2)}_{22} \\
&+ \gamma M^{(1)}_{23} M^{(2)}_{32}\big]\big(\tau + M^{(1)}_{22}\gamma^*\big)/\tau^2, \\
\tilde{P}^1_{33} = {}& M^{(1)}_{13}\big[\gamma M^{(2)}_{11} M^{(1)}_{31} + \gamma M^{(2)}_{21} M^{(1)}_{32} \\
&+ M^{(2)}_{31}\big(\tau + \gamma M^{(1)}_{33}\big)\big]\gamma^*/\tau^2 + M^{(1)}_{23}\big[\gamma M^{(2)}_{12} M^{(1)}_{31} \\
&+ \gamma M^{(2)}_{22} M^{(1)}_{32} + M^{(2)}_{32}\big(\tau + \gamma M^{(1)}_{33}\big)\big]\gamma^*/\tau^2 \\
&+ \big[\gamma M^{(2)}_{13} M^{(1)}_{31} + \gamma M^{(2)}_{23} M^{(1)}_{32} + \big(\tau + \gamma M^{(1)}_{33}\big) M^{(2)}_{33}\big] \\
&\times \big(\tau + M^{(1)}_{33}\gamma^*\big)/\tau^2,
\end{aligned}$$

$$\begin{aligned}
&M^{(j)}_{11} = e^{-\theta_j}\sqrt{2}, \quad M^{(j)}_{12} = e^{-i\xi_j}\varepsilon^{(j)}_1, \quad M^{(j)}_{13} = e^{-i\xi_j}\varepsilon^{(j)}_2, \\
&M^{(j)}_{21} = e^{i\xi_j}\varepsilon^{*(j)}_1, \quad M^{(j)}_{22} = e^{\theta_j}/\sqrt{2}, \quad M^{(j)}_{23} = 0, \\
&M^{(j)}_{31} = e^{i\xi_j}\varepsilon^{*(j)}_2, \quad M^{(j)}_{32} = 0, \quad M^{(j)}_{33} = e^{\theta_j}/\sqrt{2},
\end{aligned}$$

where $j = 1,2$ and

$$\begin{aligned}
\theta_j &= 8\alpha_j\beta_j t + 2x\beta_j - 2\delta_j, \\
\xi_j &= 4\big(\alpha_j^2 - \beta_j^2\big)t + 2x\alpha_j - 2\chi_j.
\end{aligned}$$

It should be mentioned that the densities of the two modes are connected by the relation $|\varepsilon^{(j)}_1|^2 + |\varepsilon^{(j)}_2|^2 = 1$ $(j = 1,2)$.

III. RESULTS AND DISCUSSION

Figure 1 shows the intensity distribution in the coupled NLS equations while the contour plot displayed in Fig. 2 shows their trajectories. When one changes the strengths of SPM and XPM, one observes a rotation of the trajectory of the bright solitons in addition to the intensity distribution between the two modes as shown in Fig. 3. The contour plot shown in Fig. 4 confirms this observation. The angle of rotation of the trajectories can be further changed by varying the parameters a and b as shown in Fig. 5, and the corresponding contour plot is displayed in Fig. 6. Comparing the density profiles shown in Fig. 1 with Figs. 3 and 5, one understands that in addition to the rotation of trajectories of bright solitons, one also witnesses a realignment of intensity distribution between the modes ψ_1 and ψ_2. The rotation of the trajectories of bright solitons arises due to the extra energy that is being pumped into the dynamical system by varying the SPM and XPM parameters. This excess energy contributes not only to the rotation, but also to the realignment of intensity distribution.

It should be mentioned that the rotation of the trajectory of bright solitons is witnessed in the modified coupled NLS equations themselves. For the intensity profile of the modified coupled NLS equations shown in Fig. 7, one observes shape-changing collisional dynamics of bright solitons similar to that in the coupled NLS equations. In addition, the trajectory of bright solitons is diagonally opposite (as shown in Fig. 8) to that observed in the coupled NLS equations (Fig. 2). The angular separation between the bright solitons can also be changed as desired by manipulating the complex hidden spectral parameter μ as shown in Figs. 9 and 10. It is worth noting that the variation of the angular separation of bright solitons occurs in the coupled NLS equations themselves. From the above, one understands that the variation of SPM or XPM parameters injects extra energy into the dynamical system which results not only in the rotation of the trajectories of the bright solitons, but also in the realignment of their intensity distribution.

IV. CONCLUSION

In summary, the collisional dynamics of bright solitons in the coupled NLS equations shows that apart from the intensity redistribution, one witnesses the rotation of the trajectories of bright solitons and realignment of intensity distribution between the two modes by varying the self-phase-modulation or cross-phase-modulation parameters. In addition, the angular separation between the bright solitons can also changed suitably. We believe that these results may stimulate a lot of experiments in nonlinear optics, Bose-Einstein condensates, and left- right-handed metamaterials.

ACKNOWLEDGMENTS

The authors thank the referee for invaluable suggestions. They would like to express their gratitude to Professor M. Lakshmanan for his suggestions. P.S.V. wishes to thank UGC and DAE-NBHM for financial support. R.R. wishes to acknowledge the financial assistance received from DAE-NBHM [Grants No. 48(1)/NBHM/-R and No. D II/ 4524], UGC [Grant No. F.No 40-420/2011(SR)], and DST (Grant No. SR/S2/HEP-26/2012). K.P. acknowledges DST and CSIR, Government of India, for financial support through major projects.

[1] A. Hasegawa and F. Tappert, Appl. Phys. Lett. **23**, 142 (1973); **23**, 171 (1973).

[2] L. F. Mollenauer, R. H. Stolen, and J. P. Gordon, Phys. Rev. Lett. **45**, 1095 (1980).

[3] G. P. Agarwal, *Nonlinear Fibre Optics*, 5th ed. (Academic Press, Oxford, UK, 2012).

[4] N. E. Zakharov and E. I. Schulman, Physica D **4**, 270 (1982); R. Sahadevan, K. M. Tamizhmani, and M. Lakshmanan, J. Phys. A **19**, 1783 (1986).

[5] N. Akmediev and A. Ankiewicz, *Solitons: Nonlinear Pulses and Beams* (Chapman & Hall, London, 1997); C. R. Menyuk, IEEE J. Quantum Electron. **23**, 174 (1987); M. Wadati, T. Iizuka, and M. Hisakado, J. Phys. Soc. Jpn. **61**, 2241 (1992); K. Porsezian and K. Nakkeeran, Pure Appl. Opt. **6**, L7 (1997); M. Hisakado, T. Iizuka, and M. Wadati, J. Phys. Soc. Jpn. **63**, 2887 (1994).

[6] S. V. Manakov, Zh. Eksp. Teor. Fiz. **65**, 505 (1973) [Sov. Phys. JETP **38**, 248 (1974)].

[7] D. J. Kaup and B. A. Malomed, Phys. Rev. A **48**, 599 (1993); F. Kh. Abdullaev and E. N. Tsoy, Physica D **161**, 67 (2002).

[8] R. Radhakrishnan, M. Lakshmanan, and J. Hietarinta, Phys. Rev. E **56**, 2213 (1997); R. Radhakrishnan and M. Lakshmanan, J. Phys. A **28**, 2683 (1995); M. Hisakado and M. Wadati, J. Phys. Soc. Jpn. **64**, 408 (1995); R. Radhakrishnan and M. Lakshmanan, Phys. Rev. E **60**, 2317 (1999).

[9] V. G. Makhankov, N. V. Makhaldiani, and O. K. Pashaev, Phys. Lett. A **81**, 161 (1981); T. Kanna, E. N. Tsoy, and N. Akhmediev, *ibid.* **330**, 224 (2004).

[10] E. N. Tsoy and N. Akhmediev, Opt. Commun. **266**, 606 (2006).

[11] Mohammed F. Saleh and Fabio Biancalana, Phys. Rev. A **87**, 043807 (2013).

[12] David Feijoo, Angel Paredes, and Humberto Michinel, Phys. Rev. A **87**, 063619 (2013).

[13] Bettina Gertjerenken, Thomas P. Billam, L. Khaykovich, and Christoph Weiss, Phys. Rev. A **86**, 033608 (2012).

[14] K. Nakkeeran, K. Porsezian, P. Shanmugha Sundaram, and A. Mahalingam, Phys. Rev. Lett. **80**, 1425 (1998).

[15] R. H. Enns and S. S. Rangnekar, IEEE J. Quantum Electron. **23**, 1843 (1987); G. Cancellieri, F. Chiaraluce, E. Gambi, and P. Pierleoni, J. Opt. Soc. Am. B **12**, 1300 (1995).

[16] L.-L. Chau, J. C. Shaw, and H. C. Yen, J. Math. Phys. **32**, 1737 (1991).